

DEVELOPMENT OF CROSS AND PARALLEL MODE GRINDING MACHINE FOR HIGH NA ASPHERICAL MOLD AND DIE

Yuji Yamamoto¹, Hirofumi Suzuki¹, Toshimichi MORIWAKI¹, Tadashi OKINO¹,
Yoshio HIJIKATA¹, Jeffrey ROBLEE² and Tsutomu MIYASHITA³

¹ Department of Mechanical Engineering, Kobe University, Kobe, Hyogo, JAPAN

² Precitech Inc., Keene, NH, USA

³ Taylor Hobson Ltd., Shinagawa, Tokyo, JAPAN

1. INTRODUCTION

Needs of the digital camera and the mobile phone with camera increase, and the necessity of a micro and high NA aspheric glass lens has been increased in recent years. Such micro aspheric glass lenses of high NA must be molded with ceramic dies and molds made of tungsten carbide, and that are ultra-precision ground with aspherical grinding machine with micro diamond wheel. Moreover blue lasers have been increasingly used to make wavelengths short and the maximum tangent angle of the aspheric shape has increased. Therefore ultra-precision grinding technology of ceramic dies became to be a core technology. There are the cross-grinding method and the parallel-grinding method in the micro aspherical grinding. In the cross-grinding, where the wheel rotational direction is cross to the workpiece rotational direction, form accuracy and surface roughness are usually fine compared with the parallel-grinding. In the recent digital cameras or mobile phone with lenses many aspherical lenses have to be install. In some aspherical shape, parallel-mode grinding is superior in precision grinding. Because in that case the grinding wheel with large diameter and small tip radius can be used, the wheel wear can be reduced and workpiece form deviation can be increased. Then grinding machine with the cross mode and parallel mode grinding has been required.

2. MICRO ASPHERICAL GRINDING

2.1 Problem of the cross grinding

Most of the aspherical grinding, the cross-grinding is usually used because of its superior ground surface. But in some aspherical shape such as high NA lens, small radius r_t of the wheel must be used to contact to the minimum local workpiece curvature in case of the cross grinding as shown in Fig.1 (a).

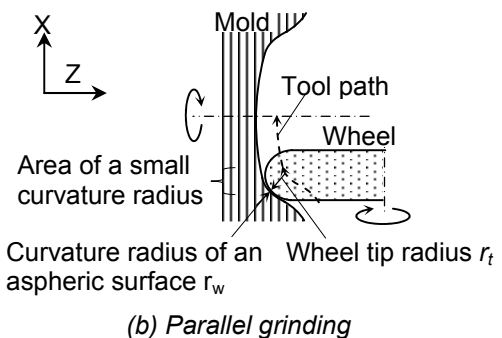
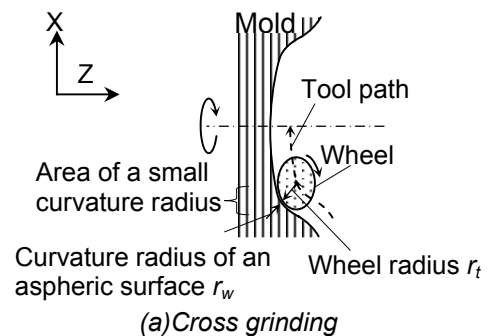


Figure 1: Grinding of an aspherical surface

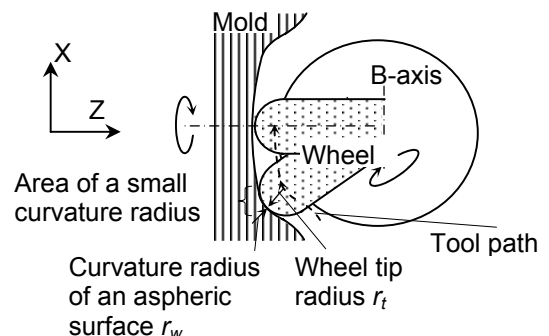


Figure 2: The illustration of the simultaneous 3 axis (X, Z, B) controlled parallel grinding method

In this case, the grinding area on the workpiece A_w becomes much larger than that on the wheel

A_t (Wheel diameter $\times \pi \times$ contact width), then the wheel wear will be large and it will be difficult to obtain a fine form accuracy.

2.2 Parallel-grinding

Then in this case, the parallel-grinding must be applied to use large diameter of the wheel. The wheel tip radius r_t must be smaller than the minimum local workpiece curvature, however a large radius wheel can be used as shown in Fig.1 (b). Then the wheel wear can be decreased.

However, the waviness and surface roughness of the wheel surface are completely transferred to the workpiece surface, and then it is necessary to true or form the wheel surface smoothly with so much truing process in order to obtain the superior wheel surface. Furthermore, the workpiece form accuracy will become large because of the unequal distribution of wheel wear. In order to improve these problems, a rotary B axis has to be added to the grinding machine and grinding point on the wheel surface will be fixed as shown in Fig.2.

In this study, the ultra-precision grinding machine of simultaneous 3-axes (X, Z, B) control was developed. Moreover, although the conventional rotational axis had insufficient positioning accuracy, the rotational axis of new oil hydrostatic pressure slide was developed to be used as a B axis.

3. GRINDING MACHINE/SYSTEM

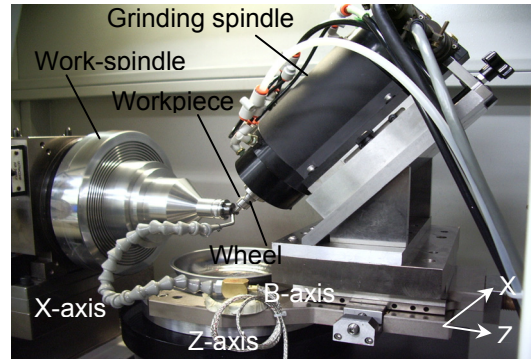
A view of the grinding machine is shown in Fig. 3. The specifications of the machine are shown in Table 1. The grinding wheel was actuated with X, Z linear motor driven tables of 8.4 nm (X, Z) in positioning resolution. B axis rotary table is the oil hydrostatic rotary table with high stiffness and high resolution in the wedge. In the grinding experiments, the aspherical workpiece was vacuum chucked with the jig onto the workpiece air spindle. The grinding wheel was installed to 45 degrees tilted and high-speed spindle with collet chuck and the grinding spindle was set on the B-axis rotary table. Each axis was controlled with PC based NC system. The cross-grinding mode or parallel grinding modes can be selected by exchanging a jig.

4. GRINDING EXPERIMENTS

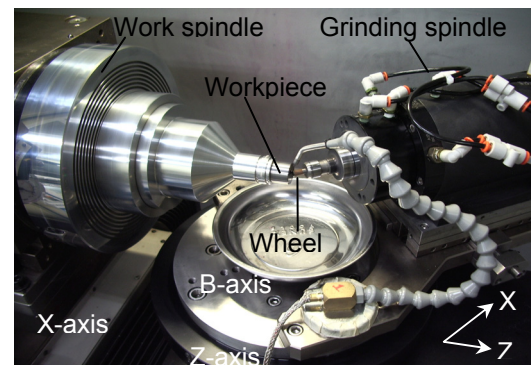
4.1 Cross-grinding

Figure 4 shows an illustration of the 45 degrees tilted grinding method. As a grinding spindle, the high speed air spindle was installed, and is driven by simultaneous 2 axis (X,Z). A micro cylindrical type of resinoid bonded diamond

wheel was chucked into the grinding spindle with a collet chuck.



(a) Cross grinding



(b) Parallel grinding

Figure 3: Appearance of the developed grinding machine

Table 1 Specifications of grinding machine

Axes	Travel (mm)	Resolution
X	190	1.4 nm
Z	190	1.4 nm
B	Endless	1/10000 degree

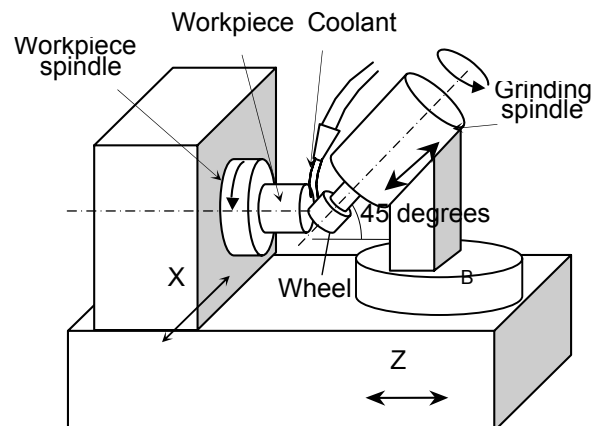


Figure 4: Cross-grinding mode of simultaneous 2 axes (X, Z) controls

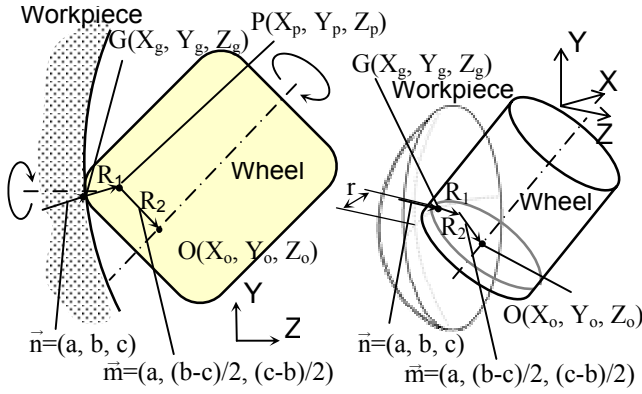


Figure 5: Tool path in cross-grinding of simultaneous 2 axis (X, Z) control

Table 2 Grinding conditions (Cross grinding)

Grinding wheel	Resinoid bonded diamond wheel
Grain size	# 1200
Diameter	2 mm
Rotational rate	40,000 min ⁻¹
Workpiece	Tungsten carbide
Rotational rate	200 min ⁻¹
Depth of cut	2 μm/path
Feed rate	0.1 mm/min
Coolant	Oil mist

(a) Wheel path

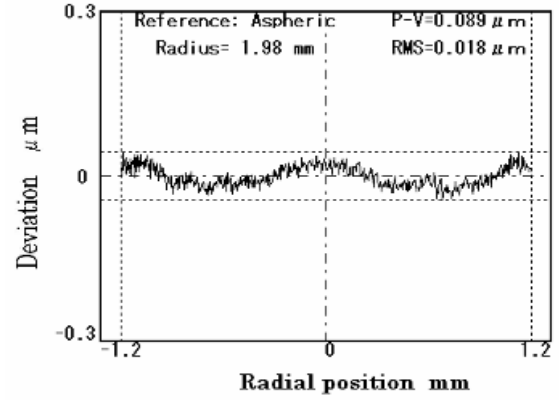
The wheel center point $O (X_o, Y_o, Z_o)$ can be obtained from the coordinate of grinding point $G (X_g, Y_g, Z_g)$ and the normal vector $\vec{n} (a, b, c)$ at the grinding point as shown in Fig. 5 by the following formulae.

$$\left. \begin{aligned} X_o &= X_g + \frac{a}{1} \cdot R_1 + \frac{a}{L} R_2 \\ Y_o &= Y_g + \frac{b}{1} \cdot R_1 + \frac{b-c}{2 \cdot L} R_2 \\ Z_o &= Z_g + \frac{c}{1} \cdot R_1 + \frac{c-b}{2 \cdot L} R_2 \end{aligned} \right\} \quad (1)$$

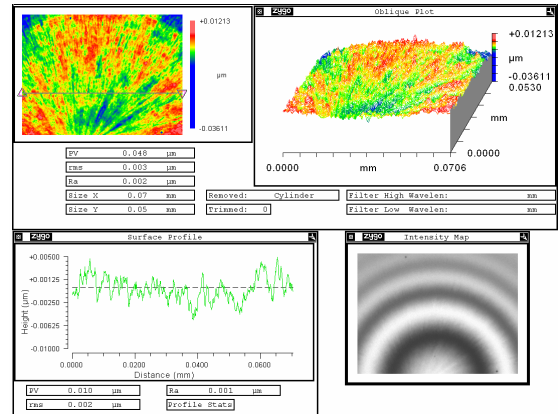
Where, $|\overline{GP}| = R_1$, $|\overline{PO}| = R_2$, $1 = \sqrt{a^2 + b^2 + c^2}$ and $L = \sqrt{a^2 + 0.5 \cdot (b-c)^2}$. Moreover, this system is actuated by 2-axes (X, Z) drives, the wheel center point (X_o, Z_o) that realize $Y_o = -R/2^{0.5}$ is calculated numerically by using Newton-Raphson method.

(b) Grinding conditions

Table 2 shows the grinding conditions. As a wheel, a resinoid bonded diamond wheel of # 1200 was used and diameter was about ϕ 2 mm.



(a) Form deviation (0.09 μmP-V)



(b) Surface roughness (10nmRy, 1nmRa)
Figure 6: Grinding results (Cross grinding)

The wheel shape was cylindrical shape and the wheel edge was trued to 0.8mm in the radius curvature. As a workpiece, molding die of 2 mm in radius curvature was tested and the material was tungsten carbide.

(c) Grinding results

Figure 6 shows a deviation profile and surface roughness profile after final grinding. The form accuracy of 0.09 μmP-V and mirror surface were obtained.

4.2 Parallel-grinding

Figure 7 shows an illustration of the parallel-grinding, which actuated by simultaneous 3-axes control X, Z, and B. Grinding spindle was set on the B axis rotary table and grinding point on the wheel was controlled to be fixed.

(a) Wheel path

The wheel center point $O (X_o, Z_o, B_o)$ can be obtained from the coordinate of grinding point $G (X_g, Z_g, B_g)$, distance from wheel tip to B axis rotation center R_{tB} and the tangential angle θ of

the grinding point, as shown in Fig. 6 and by the following formulae.

$$\left. \begin{aligned} X_o &= X_g + R_{IB} \cdot \sin \theta \\ Z_o &= Z_g + R_{IB} \cdot (1 - \cos \theta) \\ B_o &= \theta \end{aligned} \right\} \quad (2)$$

(b) Grinding conditions

Table 3 shows the grinding conditions. As a wheel, a resinoid bonded diamond wheel of # 1200 was used and diameter was about ϕ 5 mm.

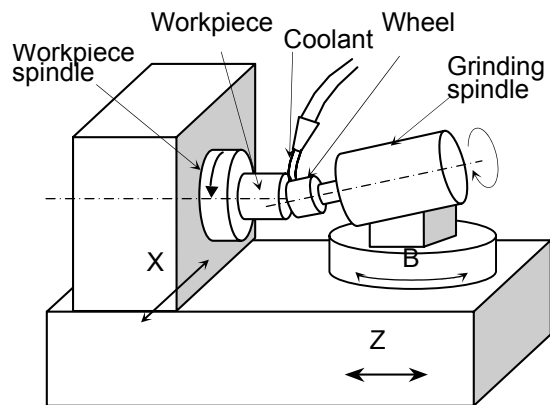


Figure 7: Tool path in parallel-grinding of simultaneous 3-axes (X, Z, B) control

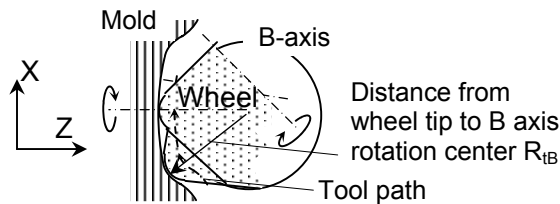


Figure 8: Parallel-grinding of simultaneous 3-axes (X, Z, B) control

Table 3 Grinding conditions (Parallel grinding)

Grinding wheel	Resinoid bonded diamond wheel
Grain size	# 1200
Diameter	5 mm
Rotational rate	40,000 min ⁻¹
Workpiece	Tungsten carbide
Rotational rate	200 min ⁻¹
Depth of cut	2 μ m/path
Feed rate	0.2 mm/min
Coolant	Oil mist

(c) Grinding results

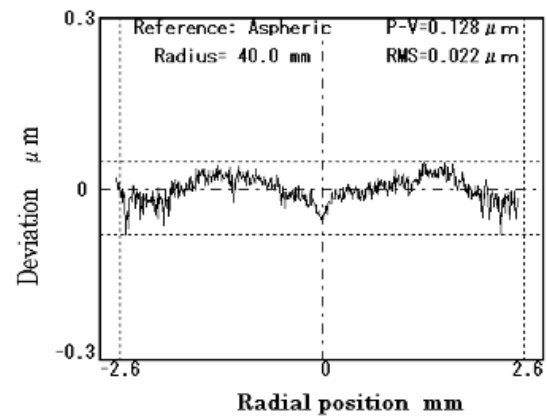
Figure 9 shows a deviation profile and surface roughness profile after final grinding. The form accuracy of 0.13 μ mP-V and mirror surface were obtained.

CONCLUSIONS

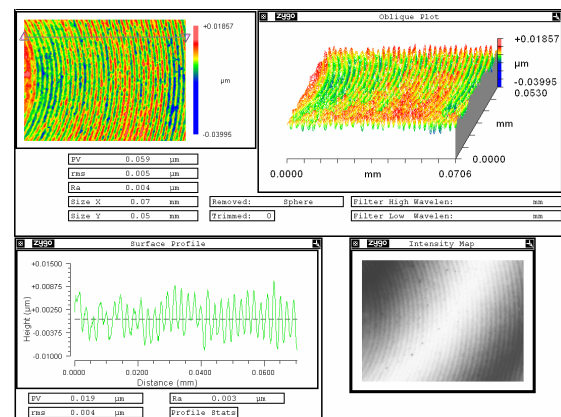
The grinding machine with crossing mode and the parallel mode was developed. As a result, the good result was obtained in the two modes.

REFERENCES

(1) Yuji Yamamoto, Hirofumi Suzuki, et al., Ultra Precision Grinding of Micro Aspherical Surface, Proceedings of 2004 ASPE Annual Meeting, FL (USA), Oct, 558-561.



(a) Form deviation (0.13 μ mP-V)



(b) Surface roughness (19nmRy, 3nmRa)
Figure 9: Grinding results (Parallel grinding)